RECONCILIATION OF LOG AND LABORATORY DERIVED IRREDUCIBLE WATER SATURATIONS IN A DOUBLE POROSITY RESERVOIR

Lucienne Bouvier, Sylvie M. Maquignon
TOTAL CFP, Paris, France

ABSTRACT Reconciliation of the irreducible water saturation measured in the laboratory on capillary pressure curves and determined in-situ by logs has been achieved by a study of the resistivity index correlated with the pore size distribution of different samples of a limestone reservoir.

The reservoir is an oolithic limestone with a bimodal pore size distribution ; three ranges of porosity are identified ; the macroporosity or intergranular porosity with large pores, the microporosity or intragranular porosity with fine pores and an intermediate porosity with pores of medium size. The distribution of these three classes of porosity is variable from one sample to another.

Resistivity index variation versus water saturation was determined, with corresponding capillary pressure curves, using the porous plate method on a water-oil system, oil being dead crude oil. Afterwards, mercury injection was carried out on the same samples in order to get the pore size distributions.

Using an appropriate transposition factor, the capillary pressure curves obtained by both methods are shown to be quite similar, except in the low capillary pressures portion. In this part, water oil curves are below the mercury curves due to the slight oil wettability of the reservoir. It is then possible to correlate the water saturation variations with the pore sizes.

The variation of the resistivity index with the water saturation, in a logarithmic form, shows three different slopes ; only the first one, at high water saturations, leads to an Archie value of n around 2. The slope variations are observed for water saturations correlating with the successive displacements of water by oil in the three classes of porosity.

So, the Archie value of n around 2 is only applicable to the samples that contain macroporosity and for high values of water saturation, that is in the transition zone of the reservoir. In the oil zone, the resistivity of the rock that contains water only in the microporosity is much higher than that predicted by the Archie law. Using n = 2 for the interpretation of the resistivity logs leads to underestimate the irreducible water saturation. This is critical in low permeability zones, i.e. where no macroporosity is detected.

INTRODUCTION

Estimation of oil-in-place within a reservoir is computed from porosity and resistivity logs using the following equation :

$$Sw = a\phi^{-m}\left[\frac{Rw}{Rt}\right]^{\frac{1}{n}}$$

derived from the two empirical relationships from Archie (1942)

$$F_R = \frac{Ro}{Rw} = a\phi^{-m}$$

and

$$I_R = \frac{Rt}{Ro} = Sw^{-n}$$

where

F_R = formation factor

I_R = resistivity index

Rw = electrical resistivity of the formation brine

Ro	=	electrical resistivity of the reservoir rock fully saturated with the formation brine
Rt	=	electrical resistivity of the reservoir rock at a water saturation Sw
ϕ	=	porosity
m	=	cementation exponent
n	=	Archie's saturation exponent

The application of this equation with a=1, m=2 and n=2, as determined by Archie, is valid only for strongly water-wet consolidated rocks, free of clays and for water saturation higher than 0.15.

Since then, many corrections have been supplied to obtain a more general equation. So, correcting terms are used to take into account the electrical effects of shaliness (Waxman et al.1968 ; Clavier et al.1977).

The values of a and m are either determined from empirical correlations or obtained from laboratory tests ; a is generally close to 1 but m varies with the consolidation of the rock.

As far as the second Archie equation is concerned, the saturation exponent has been found much smaller than 2 for tight sandstones (de Waal et al, 1989) and limestones (Dixon et al, 1990) ; n can also be significantly higher than 2 in oil-wet rock as shown in the bibliographic review made by Anderson (1986) or Mahmood et al (1988). Finally, an increasing number of cases are being encountered where the saturation exponent has been observed to change with variation in fluid saturation within a given rock (Diederix, 1982 ; Swanson, 1985 ; Rasmus, 1986 ; de Waal et al, 1989 ; Longeron et al, 1989 ; Worthington et al, 1990). Almost all rocks studied are sandstones and the explanation for a variable n is the existence of a multimodal pore size distribution. For example, this phenomenon was observed in presence of microporosity inside clays like kaolinite, but also when the effect of shale was negligible.

The purpose of this paper is to present another case of non linear relationship between I_R and Sw, on a double-logarithmic scale, observed on a limestone reservoir. A dependence of saturation exponent on water saturation was detected in a systematic study undertaken to explain the large discrepancy between the irreducible water saturation obtained from logs using Archie's laws and the

irreducible water saturation measured in special core analysis. The measurement of wettability, electrical indexes and capillary pressure curves was performed. It was possible to correlate changes in n values with pore size distribution and to derive an empirical relationship for the calculation of water saturation from logs.

ROCK DESCRIPTION

The reservoir is an oolithic limestone which porous network is composed of intergranular porosity localized between the ooïds, in competition with intercrystalline porosity associated with cementation and of intragranular porosity inside the ooïds more or less connected with the other types of pores.

On the whole set of samples used for special core analysis, the average arithmetic value of porosity is around 14.5 % and the average geometric value of water permeability is around 1.5 E-15m^2. The correlation between porosity and water permeability, as shown in Figure 1, is fair with a correlation coefficient of 0.82.

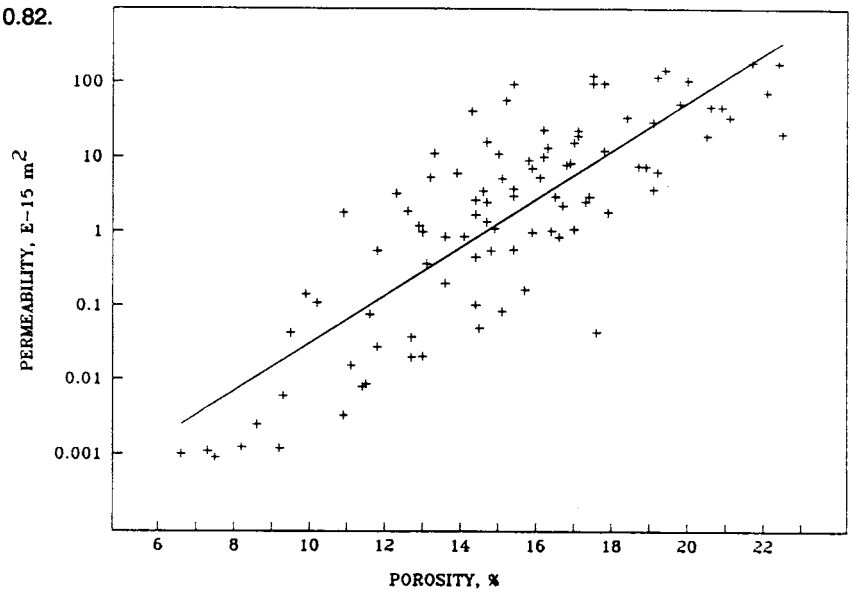

Figure 1 Water permeability-porosity correlation

EXPERIMENTS

After determination of porosity and brine permeability, the formation factor was measured on all samples without confining pressure and on a selected set of samples under overburden pressure, with a two electrodes system.

Then resistivity indexes together with the oil-water capillary pressure curve were determined using the porous plate technique, in individual cells, without confining stress. Resistivity was measured with two platinum electrodes installed at the top and at the bottom of the sample. Oil was dead crude oil from the reservoir ; it can penetrate the sample from all directions except via the end face, which is in capillary contact with the porous plate. Close increasing steps of oil pressure were applied in order to well define the I_R-Sw relationship that was suspected to have an abnormal behaviour. Couples I_R-Sw were recorded even if the equilibrium of the water saturation, at the imposed capillary pressure, was not achieved. The tests were completed with a capillary pressure up to 300 kPa or more often when breakthrough of oil occurred.

Afterwards, samples were cleaned and capillary pressure curves using the standard mercury injection method were determined.

Wettability was measured on preserved samples taken with water-base mud and on restored samples, according to the Amott/IFP procedure, using dead crude oil. The restoration procedure consists in ageing, at reservoir temperature, the sample at irreducible water saturation established by flooding with dead crude oil after cleaning and brine saturation.

RESULTS

Formation factor

The average value of cementation exponent m is 1.95 without confining pressure ; it becomes 2.02 when including the effect of overburden pressure.

Wettability

The reservoir rock is slighly oil-wet, with a wettability index around -0.2. This index was measured on preserved samples, taken with water-base mud. The negative value results from the absence of spontaneous imbibition by water and a slight spontaneous imbibition by oil. The same wettability index was found on the restored samples. This confirms that there is probably no artefact due to wettability in the resistivity index measurement because of the same cleaning procedure and the use of dead crude oil as for the restoration, the only difference being the temperature during ageing.

Pore size distribution

Some characteristic examples of the results derived from the mercury capillary pressure curves are presented in Figures 2 and 3. The differential pore entry size distribution is given in Figure 2 and the porosity distribution versus the pore entry size is given in Figure 3. The diameter of the pore entries was calculated using :

$$d = \frac{\sigma \cos\theta}{P}$$

where

σ = 490 mN/m (mercury-vacuum interfacial tension)

θ = 140°

P = mercury capillary pressure

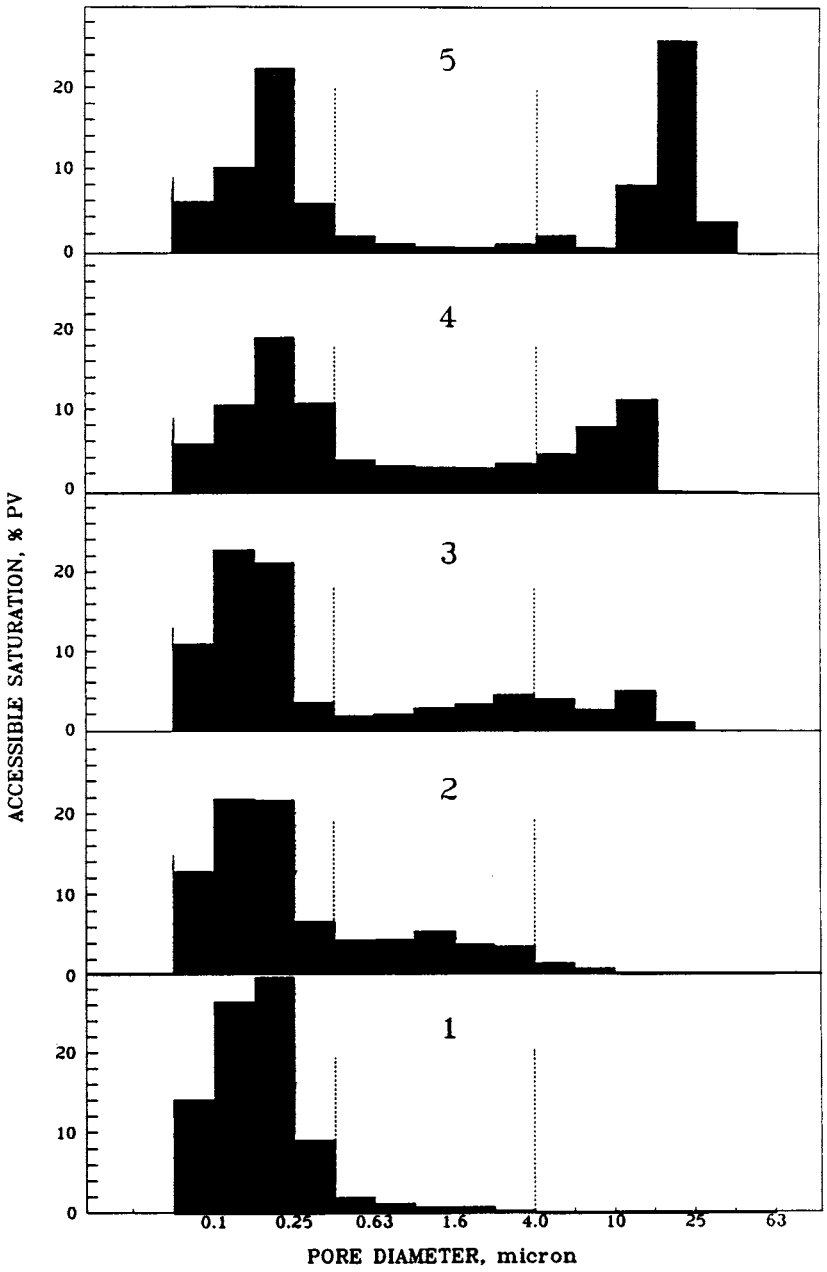

Figure 2 Pore size distribution

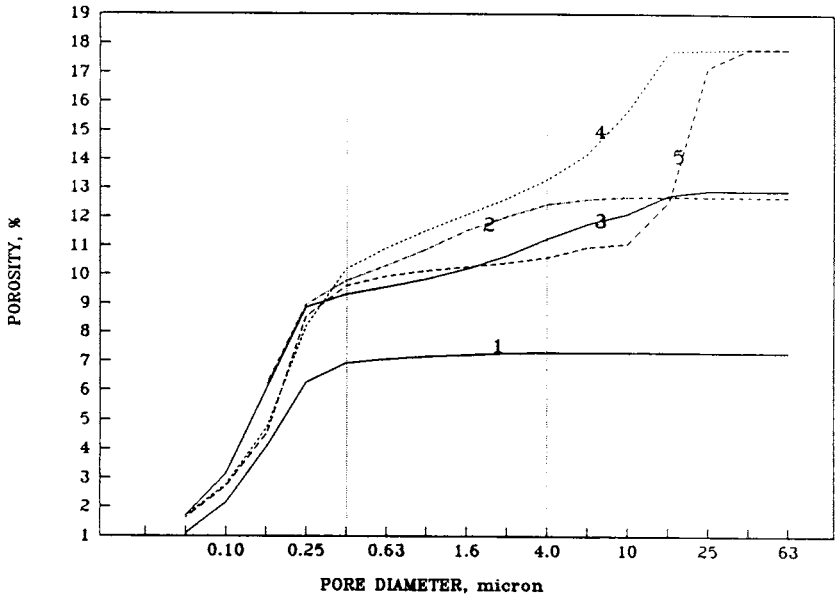

1 : Kw = 0.001 E-15 m^2 - 2 : Kw = 0.02 E-15 m^2
3 : Kw = 1.17 E-15 m^2 - 4 : Kw = 12.0 E-15 m^2
5 : Kw = 95.3 E-15 m^2

Figure 3 Porosity distribution

Samples show a bimodal pore size distribution with macro, intermediate and microporosity. The cuts between the three porosities for all samples are always around 0.4 μ and 4.0 μ. But the distribution of these three classes of porosity is variable from one sample to another. Sample 1 contains only microporosity, sample 2 micro and intermediate porosity but no macroporosity, samples 3, 4 and 5 contain the three classes but at different levels ; 3 has very few macroporosity, 5 has much macroporosity and very little intermediate and sample 4 has an equivalent amount of macro and intermediate porosity. All analyzed samples belong to one of different types described above. Obviously, the water permeability is fairly correlated with the fraction of macro plus intermediate porosity :

$$\log Kw = 0.099\, f - 3.37$$

where f = % pores of diameter higher than 0.4 μ

with a correlation coefficient of 0.86

Although pore diameters derived from mercury injection do not represent the actual dimensions of the throats between pores, the three classes of porosity are certainly linked to the intergranular, intercrystalline and intragranular porosity observed by thin section analysis.

Water-oil capillary pressure curves

The capillary pressure curves, together with the resistivity index were determined only on samples of enough permeability. Results obtained from three characteristic samples (3-4 and 5) are presented in Figure 4.

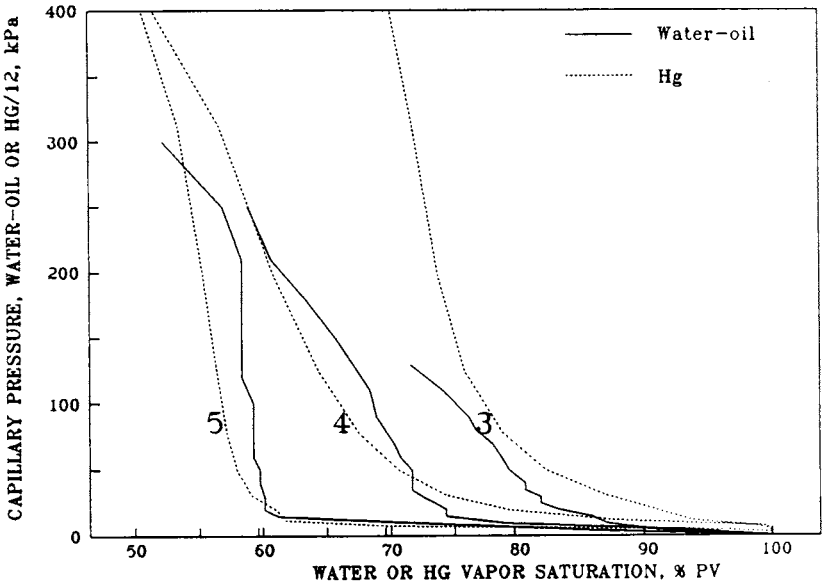

Figure 4 Capillary pressure curves

Three phases of water displacement by oil are visible :

- the first one, at low level of capillary pressure, where water saturation decreases rapidly for a low variation of capillary pressure, corresponds to the invasion of the macropores

- followed by a small variation of water saturation, higher for samples 3 and 4 than for sample 5, despite a high increase in capillary pressure that may correspond to the invasion of intermediate porosity.
- and again a more important variation of water saturation with capillary pressure, for values higher than 200-250 kPa, corresponds to the invasion of microporosity.

All these observations can be made also on the mercury capillary pressure curves in Figure 4 after dividing the mercury capillary pressure by 12 ($\sigma \cos \theta_{Hg}$ = 375 mN/m ; $\sigma_{water\text{-}oil}$ = 32 mN/m). However, the water oil curves are slightly below the mercury curves at low level of capillary pressure which confirms the slight oil wettability of the rock. At high capillary pressure, the residual saturation is generally lower for mercury curves than that for water-oil curves, which can be explained by the lack of saturation equilibrium in the water-oil system eventhough tests last around six months (Swanson, 1985). Taking into account the reservoir characteristics and the ratio of interfacial tensions, the irreducible water saturation in the reservoir has to be read on the laboratory capillary pressure curves at 130 kPa resulting for the three samples in the following values :

Samples	3	4	5
Residual saturation by mercury, %	76.1	64.5	56.8
Water residual saturation, %	71.9	67.5	58.8

These values represent a lower and an upper limit of the actual irreducible water saturation.

Resistivity index

The curves of resistivity index versus water saturation, on a double logarithmic scale, presented in Figure 5 for samples 3, 4 and 5 are characteristic of the curves obtained for the whole set of the 15 studied samples.

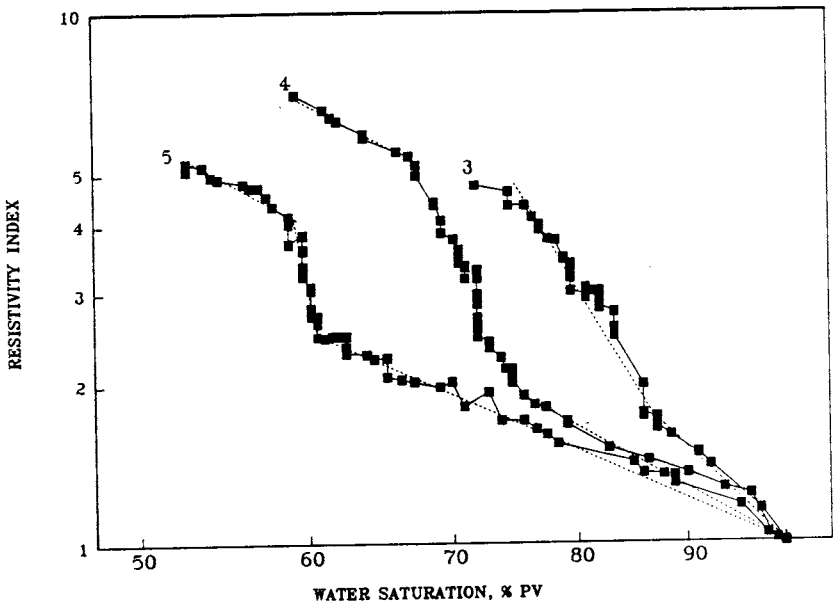

Figure 5 Resistivity index

The resistivity index curve can be divided in approximately three straight-line segments with three different slopes. The first segment at high values of water saturation has a slope close to 2, with a trend towards higher values when permeability decreases. The first slope change occurs at variable water saturation according to sample, but that corresponds always, if reported on water-oil capillary pressure curve, to a capillary pressure of about 30 kPa. The second segment has a very high slope value and is almost vertical for sample 5 and for all samples that contain only few intermediate porosity. The second slope change is observed when water saturation reaches the value that corresponds to a water-oil capillary pressure of about 200 kPa. The third segment with a small slope value, of no practical interest because of the high capillary pressure, was previously observed as single response when trying to measure resistivity index on low permeabilities samples that contain only microporosity. These three straight-line segments correspond a priori to the three phases of displacement of water by oil observed with the capillary pressure curves : invasion of macro, intermediate and microporosity respectively.

The value of water saturation Sw1 at which the first slope change occurs on each resistivity index curve and the value of irreducible water saturation Swi, at a capillary pressure of 130 kPa, on each water-oil capillary pressure curve, were recorded. Since the mercury and water-oil capillary pressure curves are very close, as shown above, it is possible to deduce from the mercury capillary pressure curves, the pore entry diameters in which oil has displaced water at the first slope change and at Swi, by assuming that these two particular water saturations are equivalent to vapor saturations from the mercury capillary pressure curves. On all samples, it was noted that the first slope change occurs when oil has displaced water in all the pores of diameter higher than about 4μ and that, at Swi, water remains only in pores of diameter lower than 1μ, as shown by the two following correlations :

$Sw1 = 0.955\ S4\mu + 1.25$ with a correlation coefficient of 0.84

$Swi = 0.828\ S1\mu + 10.6w$ with a correlation coefficient of 0.74

where $S4\mu$ = vapor saturation from mercury injection at capillary pressure corresponding to a pore entry diameter of 4μ, in per cent

$S1\mu$ = vapor saturation from mercury injection at a capillary pressure corresponding to a pore entry diameter of 1μ, in per cent.

In conclusion, the behaviour of saturation exponent is well correlated with the invasion by oil of the three different classes of porosity. When water saturation decreases in the macropores of diameter higher than 4μ, the resistivity index obeys Archie's law but with a saturation exponent n comprised between 2 and 3, in accordance with the behaviour of an oil-wet rock. When all displaceable water in macropores is replaced by oil, the resistivity index increases abruptly which is highly significative of an important decrease of continuous path for water conductance, specific again of an oil-wet rock. This phenomenon, seldom experimentally shown, takes place until capillary pressure is sufficiently high to allow oil to penetrate micropores. Then water drains with very little influence on resistivity resulting in a low slope.

Table 2 Summary of laboratory data

Well Depth (Core)(ft)	Depth (log)	Pressure (psi)	Porosity (fraction)	Vp (ft/sec) (Water sat)	Vs (ft/sec) (Water sat)	Pois. Ratio (dynamic) (undrained)	Pois. Ratio (dynamic) (drained)	Pois. ratio (static)	Cp (1/psi) (dynamic) (drained)	Cp (1/psi) (static) (test)	Youngs Mod. (dynamic) (drained)	Youngs Mod. (Static) (psi)
WELL A 4" (Vertical full diameter sample)												
X746	X765	4000	0.16	13404	8028	0.22	0.142		2.83E-06		4.73E+06	
X747	X766	4000	0.163	13257	8000	0.214	0.126		2.98E-06		4.62E+06	
X748	X767	4000	0.132	14109	8407	0.225	0.163	0.144	2.66E-06	1.27E-05	5.38E+06	1.18E+06
X749	X768	4000	0.156	13450	8008	0.225	0.151		2.82E-06		4.76E+06	
X750	X769	4000	0.157	13201	7957	0.214	0.121		3.17E-06		4.57E+06	
X751	X770	4000	0.161	13767	8097	0.235	0.181	0.158	2.39E-06	1.00E-05	4.97E+06	1.16E+05
WELL B 2 3/4" (Vertical full diameter samples)												
X687	X695	4000	0.131	13950	8362	0.219	0.146	0.115	3.09E-06	1.08E-05	5.25E+06	1.47E+06
X703	X711	4000	0.157	13684	8181	0.222	0.154	0.151	2.65E-06	7.67E-06	4.98E+06	1.55E+06
X728	X751	4000	0.126	13967	8207	0.234	0.173	0.137	3.0E-06	1.02E-06	5.2E+06	1.50E+06
X794	X803	4000	0.161	13233	7674	0.247	0.182	0.189	2.65E-06	6.13E-06	4.47E+06	1.64E+06
X831	X840	4000	0.146	13502	7769	0.252	0.194	0.176	2.69E-06	8.63E-06	4.68E+06	1.37E+06
X913	X920	4000	0.12	14352	8473	0.233	0.177	0.175	2.90E-06	7.82E-06	5.58E+06	1.78E+06
X931	X938	4000	0.13	14247	8318	0.241	0.193	0.182	2.62E-06	7.25E-06	5.41E+06	1.73E+06
WELL B 1 1/2" (Vertical plug samples)												
X930	X936	4000	0.11	15165	8812	0.256	0.214		2.49E-06		6.21E+06	
X883	X841	4000	0.155	13291	7868	0.23	0.153		2.92E-06		4.60E+06	
X729	X752	4000	0.139	14106	8021	0.257	0.215		2.38E-06		5.16E+06	
X692	X700	4000	0.082	15892	9475	0.224	0.19		3.13E-06		7.24E+06	

Pressure (confining pressure of velocity measurements, in psi).
Porosity (porosity of the core at the above confining pressure).
Vp (compressional acoustic velocity in feet/second as measured on brine saturated cores).
Vs (shear acoustic velocity in feet/second as measured on brine saturated cores).
Poisson's ratio (dynamic, undrained) Poisson's ratio calculated from raw acoustic velocities.
Poisson's ratio (dynamic, drained) Poisson's ratio calculated from corrected acoustic velocities.
Poisson's ratio (static) Measured Poisson's ratio from triaxial tests.
Cp (dynamic, drained) Pore compressibility calculated from corrected velocities, in 1/psi.
Cp (static test) Measured pore compressibility from bulk volume triaxial test, in 1/psi.
Young's mod. (dynamic, drained) Young's modulus calculated from corrected velocities, in psi.
Young's mod. (static) Measured Young's modulus from triaxial test, in psi.

RESULTS

Table 2 summarises the data collected from all sources. Only data measured at the in-situ stress value of 4000 psi are shown in this table.

Acoustic Velocity Data Integration

Figures 8 and 9 show crossplots of acoustic velocity as a function of compaction-corrected porosity for both compressional and shear modes. The data indicates excellent compatibility between laboratories. Further good trends between velocity and porosity are evident from these figures, and linear regression analysis yields the following velocity-porosity transforms for Rotliegendes sandstone. Correlation coefficients of 0.89 and 0.82 for compressional and shear regressions, respectively, were observed.

$$Vp\ (ft/sec) = 18261 - 30850\phi \quad (1)$$

$$Vs\ (ft/sec) = 10674 - 17427\phi \quad (2)$$

Extrapolation of the data to 0% porosity yields ostensibly correct sandstone matrix travel time values of 54.7 μsec/ft for compressional waves, 93.7 μsec/ft for shear waves, and a Vp/Vs ratio of 1.71.

Integration of depth-shifted core acoustic velocity and log acoustic velocity-measurements shows an excellent agreement, as illustrated by Computer-processed interpretations (CPI) in Figures 10 and 11. Core velocity data are plotted as discrete data in the same track as the wireline LSAL (Mobil Long Spaced Acoustic Log) for compressional data and SWAL (Mobil Shear Wave Acoustic Log) for shear data. Figure 10, well A, shows a 6ft block coverage of core data, which was designed to evaluate any lack of resolution or data averaging by the acoustic log when integrated with the core data. An examination of the data shows extremely good agreement between the data sets. One data point X748 (Table 2) appears to be anomalous. On close examination of this section of whole core, a 2" tight stringer runs perpendicular to the core axis, which clearly was not resolved by the acoustic log. This indicates that core sample measurement density should be increased in cases where formations show inhomogeneity. An arithmetic mean of the core and log travel time data over this 6 feet gave 72.89 μsec/ft and 73.5 μsec/ft respectively, including the anomalous point. This represents a difference of only 1.3%

But at a laboratory capillary pressure of 130 KPa which is the equilibrium pressure of Swi establishment in the reservoir, the microporosity is not reached. Consequently, the logs exploitation has to be carried out with a resistivity index obtained from the second segment of the resistivity index curve where Archie's law is no more satisfied. This appears as a difficult task since the curves are well correlated with the pore size distribution which is variable from one sample to another. This is the reason why, it was tried to establish a more general law, even approximative, based on the water permeability knowing that it is fairly correlated with the porosity which is accessible by logs.

EXPLOITATION

In order to establish that law, the following steps were applied :

1. Check that the correlation between Swi and S1μ was always valid, or improved when including all the available measured values aside from those in the present study. This was to confirm the equivalence described above between S4μ and Sw1 which is not accessible outside this study.

2. Supported by the preceeding confirmation, make sure that S4μ (in place of Sw1) and Swi were enough correlated with water permeability, using all available data.

3. Establish a correlation between the water permeability and the value of n, the slope of the first segment of the resistivity curve, and between the water permeability and the punctual value of n* at Swi calculated using :

$$n^* = \frac{-\log (I_R \text{ at SWI})}{\log (SWI)}$$

The results are presented in Table 1.

TABLE 1 Correlations for the establishment of a general law

Step	*Correlation*		*Correlation coefficient*	*Number of data*
1.	Swi	= 0.958 S1μ + 4.64	0.88	25
2.	Swi	= -9.00 logKw + 76.2	0.94	36
	S4μ	= -8.57 logKw + 79.9	0.91	50
3.	n	= -0.57 logKw + 3.11	0.69	15
	n*	= -0.93 logKw + 4.96	0.58	15

Saturations are expressed in percent and Kw in E-15m^2

Correlations are strong except for n and especially n*. Nevertheless they allow to calculate an average resistivity index curves composed of two straight-line segments for each permeability as presented in Table 2 and shown in Figure 6.

TABLE 2 Resistivity index from the new law

Permeability E-15 m^2	*Up to the slope change at Sw1 Sw1=-8.57logKw+79.9 n=-0.57logKw+3.11*			*Punctual value at Swi Swi=-9.00logKw+76.2 n*=-0.93logKw+4.96*		
	Sw1	*n*	I_R	*Swi*	*n**	I_R
100	62.7	1.97	2.51	58.2	3.10	5.35
20	68.7	2.37	2.43	64.5	3.75	5.18
10	71.3	2.54	2.36	67.2	4.03	4.96
5	73.9	2.71	2.27	69.9	4.31	4.68
1	79.9	3.11	2.01	76.2	4.96	3.85
0.1	88.4	3.68	1.57	85.2	5.89	2.57

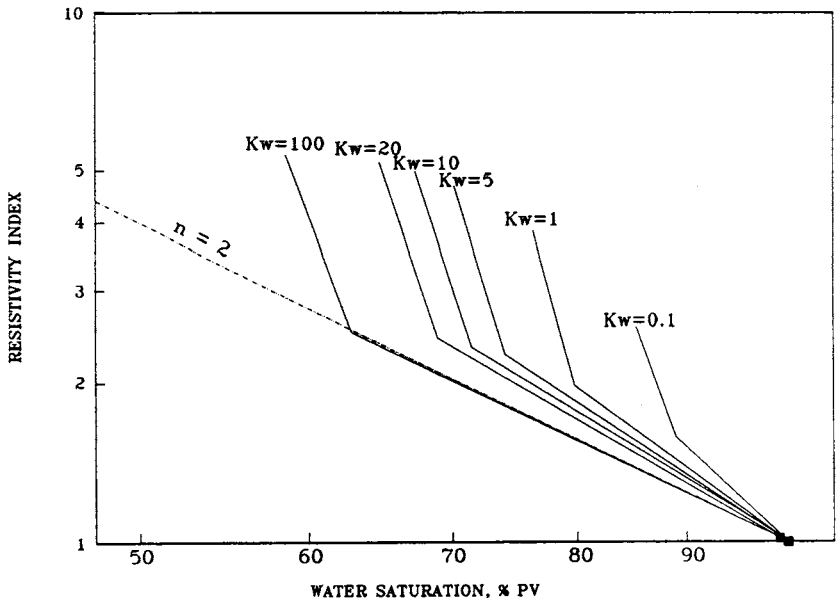

Figure 6 Resistivity index from the new law

The first straight line segment allows the computation of water saturation in the transition zone and the values of n* the computation of the irreducible water saturation. The increase of Swi is important, especially in low permeability zones. For example, for a 100 E-15m^2 sample, if in-situ Swi was determined according to Archie (m=2, n=2) to be 30 %, it becomes 46 % and for a 1 E-15m^2 sample of 45 % of Archie in-situ Swi, the new value is 72.5 %.

Despite all the approximations, results derived from this new law appear to be correct because they lead to the reconcillation of the irreducible water saturation measured in the laboratory and determined in-situ by logs as shown by the two examples given in Table 3. The in-situ values are derived from the porosity and resistivity logs using the porosity - permeability correlation and the laboratory values are measured by capillary pressure curves.

TABLE 3 Irreducible water saturation

Laboratory value	*In-situ values*	
	Archie law $m = 2, n = 2$	*New law*
69.1	26.1	68.8
76.9	37.6	73.6

CONCLUSIONS

1. Mercury injection tests have shown the variable distribution of porosity from one sample to another between macropores of diameter higher than 4μ, micropores of diameter lower than 0.4μ and pores of intermediate size.

2. The oolithic limestone reservoir is slightly oil-wet according to Amott/IFP test.

3. Mercury capillary pressure curves, using a transposition factor of 12, are close to water-oil capillary pressure curves. At low levels of capillary pressure, water-oil curves are below mercury curves confirming the slight oil wettability. The shapes of the curves are consistent with the successive displacements of water by oil in the three classes of porosity.

4. The I_R versus Sw curve, on a bilogarithmic scale, consists in three straight-line segments. The water saturation values at which the two slope changes occur are variable from one sample to another, but well correlated with the pore size distribution.

5. The first segment of the I_R versus Sw curve, for water saturation values between Sw = 100 % and Sw1 value that corresponds, for all samples to the end of displacement of water by oil in the macropores of diameter higher than 4μ, has a slope between 2 and 3. This is consistent with Archie's law for an oil-wet reservoir.

6. For water saturations lower than Sw1, I_R increases abruptly up to the second slope change when capillary pressure is high enough to allow oil to penetrate micropores ($\leq 0.4\mu$). But in reservoir conditions, the thickness of the oil column is such that water has been displaced only in pores higher than 1μ. This means that Swi has to be computed from I_R belonging to the second segment where Archie's law is no more satisfied.

7. To better analyze logs taking into account these results an approximate law has been established. It allows to compute the value of n and thus Sw in the transition zone and the value of a punctual n* from which Swi is deduced knowing the permeability which is fairly correlated with porosity.

8. Swi obtained in that way are much larger than those computed with Archie's law (m=2, n=2) especially for low permeabilities zones ; but they are consistent with laboratory Swi.

REFERENCES

ARCHIE, G.E. (1942) The electrical resistivity log as an aid in determining some reservoir characteristics. *Trans. AIME*, vol 146, 54-67.

WASMAN, M.H. and SMITS, L.J.M. (1968) Electrical conductivities in oil-bearing shaly sands. *Soc. Petr. Eng. J.*, June, 107-122.

CLAVIER, C., COATES, G. and DUMANOIR, J. (1977) The theoretical and experimental bases for the Dual Water Model for the interpretation of shaly sands. *SPE Journal* (1984) vol.28(2) 153-159.

DE WAAL, J.A., SMITS, R.M.M., DE GRAAF, J.D. and SCHIPPER, B.A. (1989) Measurement and Evaluation of resistivity index curves. *Trans. SPWLA 30th Annual Logging Symposium* (1989), Paper II.

DIXON, J.R. and MAREK, B.F. (1990) The effect of bimodal pore size distribution on electrical properties of some middle eastern limestones. *Paper SPE 20601 presented at the SPE 65th Annual Technical Conference and Exhibition*, New Orleans, Sept 23-26, 1990.

ANDERSON, W.G. (1986) Wettability Literature Survey - Part 3 : The effect of wettability on the electrical properties of porous media. *J.P.T.*, December 1986, 1371-78.

MAHMOOD, S.M., MAEREFAT, N.L. and CHANG, M.M. (1988). Laboratory measurement of electrical resistivity at reservoir conditions. Paper SPE 18179 presented at the *SPE 63rd Annual Technical Conference and Exhibition*, Houston, Oct 2-5, 1988.

DIEDERIX, K.M. (1982) Anomalous relationships between resistivity index and water saturations in the Rotliegend sandstone. *SPWLA 23rd Annual Logging Symposium* (1982).

SWANSON, B.F. (1985) Microporosity in reservoir rocks. Its measurement and influence on electrical resistivity. *The Log Analyst* (1985) 26(6), 42-52.

RASMUS, J.C. (1986) A summary of the effects of various pore geometries and their wettabilities on measured and in-situ values of cementation and saturation exponents. *Trans. SPWLA 27th Annual Logging Symposium* (1986). Paper PP.

LONGERON, D., ARGAUD, M. and BOUVIER, L. (1989) Resistivity index and capillary pressure measurements under reservoir conditions. Paper SPE 19589 presented at the *SPE 64th Annual Technical Conference and Exhibition*, San Antonio, Oct 8-11, 1989.

WORTHINGTON, P.F. and PALLATT, N (1990) Effect of variable saturation exponent upon the evaluation of hydrocarbon saturation. Paper SPE 20538 presented at the *SPE 65th Annual Technical Conference and Exhibition*, New Orleans, Sept 23-26, 1990.